Advances in Nano Research, *Vol. 11, No. 3 (2021) 327-337*
https://doi.org/10.12989/anr.2021.11.3.327

Computational modeling for nonlinear magneto-electro-elastic responses of smart multi-phase symmetric system

Allam Maalla[1] and Jun Song*[2]

[1]*School of Engineering, Guangzhou College of Technology and business, Guangzhou 510850, Guangdong, China*
[2]*School of Civil Engineering, Shandong Jiaotong University, Jinan, 250357, Shandong, PR China*

(*Received January 14, 2021, Revised August 24, 2021, Accepted August 27, 2021*)

Abstract. This paper investigates impact of thickness stretching phenomenon on the scale-dependent behavior of nano panel in electromagnetic environment in the framework of HOSNDT. Unlike classic theories of shells and plates, the radial displacement is assumed variable along the thickness direction as summation of bending, shear and thickness stretching displacements in which the last term is assumed trigonometrically variable along the thickness direction. Generalized magneto-electro-elastic equations are derived using the virtual work principle. The main novelty of the present paper is application of thickness stretching formulation on the results. The bending results are calculated using analytical method with actuating the nano panel with initial electromagnetic potentials. An extended numerical investigation is presented to examine influence of significant parameters on the static results.
Keywords: electromagnetic potentials; higher-order shear and normal deformation theory; panel; scale-dependent theory; thickness-stretching effect

1. Introduction

Various researchers proposed new HOSDT for better description of displacement field along the thickness direction. Main aim of the new proposed theories was examination of zero out of plane shear strains at top and bottom of plates and shells. Although this theory is useful for better prediction of mechanical behavior of plates and shells, however they still include some incompleteness such as zero out of plane normal strain. To account this components, HOSNDT has been proposed. This theory proposes an additional function responsible for out of plane normal strain. In this work, this theory is developed for a cylindrical nano panel subjected to electromagneto-mechanical loads. A literature survey is presented with focus on the works related to higher-order shear and normal deformation theory, electromagnetic fields and cylindrical panels.

Atmane and Tounsi (2017) studied effect of thickness stretching as well as various patterns of porosity on the vibration, bending and buckling behaviors of the functionally graded (FG) beams resting on Pasternak's foundation. Unlike traditional theories of beams, this theory uses a thickness variable transverse displacement to cover more general conditions using a parabolic function. Effect of porosity characteristics was studied on the static bending, free vibration and buckling results of the beam. Sayyad and Ghugal (2018) examined effect of thickness stretching in the framework of trigonometric shear and normal deformation theory on the buckling static bending and free vibration analyses of multi-layered sandwich composite beams. Cosine variation of out of plane transverse shear strains was accounted in the kinematic relations to show variation along the transverse direction for satisfying the zero shear strain at top and bottom. Accuracy and trueness of the proposed theory and corresponding outputs have been confirmed using comparison with those obtained results based on higher-order shear deformation theories (HOSDTs) available in literature. Carrera *et al.* (2011) concluded on the effect of thickness stretching in the plate and shell structures made from functionally graded materials (FGMs) by correction of transverse normal strain in various HOSDTs. The results of the present formulation with various order of transverse displacement along the transverse direction have been compared with those results with constant transverse displacement. Alibeigloo and Liew (2014) developed an analytical method for 3D dynamic responses of sandwich cylindrical panels including a FG core based on Fourier series. Based on the analytical method, effect of main parameters such as in-homogeneous index, span angle, and various geometric characteristics was studied on the results.

Bodaghi and Shakeri (2012) studied dynamic analysis of SS FG piezoelectric panel subjected to time-dependent pulses through the Hamilton's principle and the FSDT. Kheroubi *et al.* (2016) investigated bending and dynamics of nanobeams using a refined hyperbolic higher-order beam theory including nonlocal parameter. Tounsi *et al.* (2013) proposed a small scale dependent shear deformable model including out of plane normal strains. It was shown that there is no need to any factor to correct changes of shear stress due to proposed theory. They investigated effect of

*Corresponding author, Ph.D.,
E-mail: ma4241286@gmail.com; z.m136873@gmail.com; songjun198298@163.com

ISSN: 2287-237X (Print), 2287-2388 (Online)

nano scale parameter, side length ratio and out of plane normal strain on the static and dynamic responses of the nanobeam. Adim and Daouadji (2016) studied bending and free vibration analyses of FG plates based on a higher order shear and normal deformation theory (HOSNDT). Based on the proposed theory, the transverse displacement was decomposed into bending, shear and thickness stretching parts. Merzouki *et al*. (2019) developed a finite element (FE) based formulation for static bending analysis of a beam in nano scale based on nonlocal Eringen theory and considering thickness stretching effect. The problem was formulated using a generalized shear deformation theory with presentation of a 3-nodes beam element. A wide parametric analysis on the effect of structural and material parameters on the bending results of nanobeam was performed. Size dependency was included in vibration analysis of nanoshells (Hashemi Kachapi 2020, Farrokhi Nia *et al*. 2020).

Belarbi *et al*. (2019) provided a layerwise finite element (FE) based formulation for dynamic study of sandwich plates using the various shear deformation theories. The sandwich plate was modeled using the various higher and lower-order shear deformation theories for core and face-sheets, respectively. Accuracy and efficiency of the proposed method was confirmed through comparison with those results available in literature based on 3D theory of elasticity. Talebizadehsardari *et al*. (2020) studied effect of out of plane normal strain on the wave propagation characteristics of curved beams reinforced by graphene nanoplatelets. The HOSNDT was used for analyzing the model. Effective material properties of GNPs reinforced curved beam was estimated using the Halpin-Tsai micromechanical model and rule of mixture for modulus of elasticity and density, respectively. A size dependent model to cover all conditions of softening and hardening including two small scale parameters was employed. Through a wide parametric analysis, effect of significant input parameters such as span angle, amount of reinforcement, number of constituent layers and various wave numbers were investigated on the results. There are some works (Zhao *et al*. 2020a, b, Chen *et al*. 2021a, b, Xu *et al*. 2019, Guo *et al*. 2021, Li *et al*. 2021, Sun *et al*. 2021, Zhuo *et al*. 2020, Feng *et al*. 2021, Wang *et al*. 2018, Yang *et al*. 2017, 2020, Zhang *et al*. 2015, 2019, Ni *et al*. 2021) on the application of nano materials subjected to electro-magnetic loads in various situations. Rezaiee-Pajand *et al*. (2018) studied nonlinear analysis of thin/thick shells using two triangular shell element including three and six nodes with seven degrees of freedom. Thickness stretching was included in the kinematic relations. Elmascri *et al*. (2020) developed a hyperbolic shear and normal deformation theory (SNDT) in order to study free vibration responses of a FG plate subjected to thermomechanical loads. Efficiency and accuracy of the present paper was justified through comparison with those three-dimensional results of literature. Ganapathi (2019) developed a novel trigonometric shear deformation theory including out of plane normal strain for dynamic analysis of a curved beam reinforced with graphene porous materials. Gupta (2020) studied effect of a HOSNDT on the dynamic responses of a FG plate resting on elastic foundation. Eringen nonlocal elasticity theory was used for dynamic analysis of nano structures in various environments (Asrari *et al*. 2020, Asghar *et al*. 2020, Bellal *et al*. 2020, Asiri *et al*. 2020).

Effect of temperature variation as well as humidity was investigated on the bending results of orthotropic cylindrical shells based on three-dimensional hygro-thermoelasticity relations by Mohamed Ali *et al*. (2016). They reduced the governing equations to some simpler forms such as generalized plane strain problem. A new HOSDT and zigzag displacement function were used for description of displacement field. Shariyat and Alipour (2017) studied elastic results of a FG circular/annular plates with a negative Poisson ratio based on a semi-analytical method. To apply various normal and shear surface tractions on the top and bottom layers, a SNDT including out of plane normal strain was employed for formulation. A wide numerical investigation was provided to study influence of negative Poisson ratio on the elastic results of plate. Higher-order Reddy's shell theory was used for free vibration analysis of isotropic cylindrical shell with SS boundary conditions by Kabir and Askar (2005) using the dynamic form of virtual work principle. Based on the proposed shear deformable model, three displacement and two rotation functions were used for kinematic relations. The efficiency and accuracy of the proposed formulation was justified through comparison of results with those results obtained using Rayleigh–Ritz, FE and FD methods. Gholami *et al*. (2020) investigated primary resonance dynamics of functionally graded cylindrical panel in nano scale using the strain gradient theory to account size dependency. Authors indicated that the present formulation may be reduced to simpler forms. As an important discussion, the results were presented in terms of various size dependent theories such as modified couple stress, modified strain gradient and classical plate theories.

Amabili and Reddy (2020) developed HOSNDT for nonlinear static and dynamic analyses of laminated composite shell. Rivera *et al*. (2016) studied large deformation analysis of a composite shell through developing a new twelve-parameter element based on finite element method to account thickness stretching. The obtained results using the new element have been compared with those results using lower-order element. Amabili (2015) studied static and dynamic analyses of isotropic and laminated doubly curved shells based on a third-order thickness and shear deformation theory considering imperfection. All nonlinear strain components have been accounted in the formulation. Alijani and Amabili (2014a) studied nonlinear forced vibration and static bending analyses of rectangular plates with accounting the nonlinearities in all rotational and normal deformations. Accuracy and importance of the proposed theory were confirmed through comparison with those results in literature. Amabili (2014) developed a geometrically nonlinear theory including third-order thickness stretching terms and higher-order shear deformation terms for large-amplitude vibration analysis of laminated doubly curved shells. Alijani and Amabili (2014b) accounted full nonlinear terms in strain-displacement relations for large-amplitude

vibration analysis of functionally graded rectangular plate based on a higher-order shear deformation theory considering thickness stretching term. Rivera *et al*. (2020) employed finite element approach for nonlinear analysis of various problems with accounting an eight node element. Accuracy and trueness of the present formulation was confirmed through comparison with results of commercial codes ABAQUS and ANSYS. Zenkour (2020a) studied thermal shock analysis of a cylindrical shell subjected to thermal and mechanical loads. Zenkour and Kutbi (2020) studied effect of continuous heat source without energy dissipation on the thermoelastic interactions in a hollow cylinder based on linear generalized Green–Naghdi thermoelasticity theory. To find the governing equations in space domain, the state space approach was employed. Barati and Zenkour (2019) studied effect of graphene nanoplatelets on the free vibration analysis of porous nanocomposite shell with different distributions of porosity. Halpin–Tsai micromechanics model and rule of mixture were used for computation of effective material properties. Zenkour (2018) studied effect of thermal shock and variable thermal conductivity on the thermoelastic analysis of a clamped axisymmetric infinite hollow cylinder based on Generalized thermoelasticity theories such as Green and Lindsay, Lord and Shulman, and coupled thermoelasticity. Zenkour (2016) presented an analytical solution for investigating effect of the hygrothermal loads on the multi-field behavior of a heterogeneous piezoelectric elastic cylinders. The cylinder was subjected to a combination of mechanical, electrical and hygrothermal loads. Zenkour (2020b) studied thermo-diffusion analysis of an isotropic cylinder under thermal flux and chemical potential impacts based on Green and Naghdi generalized thermoelasticity theory.

Author tried to summarize some more related works to the subject of the present paper with focus on the higher-order shear and normal deformation theory, cylindrical panel, and piezomagnetic materials. Based on author's knowledge, there is no work on application of HOSNDT to MEE bending results of cylindrical nano panel subjected to applied electric and magnetic potentials. Thickness stretching is included in the governing equations. Based on this theory, the total transverse deflection is assumed as combination of bending, shear and stretching parts. Third-order shear deformation theory as well as nonlocal piezomagnetoelasticity relations were used for analysis of the problem. Based on the proposed theories, the magneto-electro-elastic bending results are presented to investigate effect of nano scale parameter, applied electric and magnetic potentials and length to radius ratio.

2. Thickness-stretching formulation of piezomagnetic nano panel

This section present governing equations of a piezomagnetic nano panel subjected to electromagneto-mechanical loads in the framework of HOSNDT. This theory assumes displacement field as follows:

$$u(x,\theta,z) = u_0(x,\theta) - z\frac{\partial w_b(x,\theta)}{\partial x} - f(z)\frac{\partial w_s(x,\theta)}{\partial x}, \quad (1)$$

$$v(x,\theta,z) = \left(1+\frac{z}{R}\right)v_0(x,\theta) - \frac{z}{r}\frac{\partial w_b(x,\theta)}{\partial \theta} - \frac{f(z)}{r}\frac{\partial w_s(x,\theta)}{\partial \theta},$$

$$w(x,\theta,z) = w_b(x,\theta) + w_s(x,\theta) + g(z)\chi(x,\theta),$$

where u, v, w are displacement components along axial, circumferential and radial directions, respectively. Furthermore w_b, w_s are bending and shear parts of transverse displacements and χ is an additional functions for accounting out of plane normal strain. Based on this theory, the shape functions $f(z), g(z)$ are assumed as follows:

$$\begin{aligned} f(z) &= z - h/\pi \sin(\pi z/h), \\ g(z) &= 1 - f'(z) = cos\,(\pi z/h) \end{aligned} \quad (2)$$

The kinematic relations in cylindrical coordinate system are developed as:

$$\begin{aligned} &\varepsilon_z = \frac{\partial w}{\partial z}, \varepsilon_\theta = \frac{w}{r} + \frac{1}{r}\frac{\partial v}{\partial \theta}, \varepsilon_x = \frac{\partial u}{\partial x}, \\ &\gamma_{z\theta} = \frac{1}{r}\frac{\partial w}{\partial \theta} + \frac{\partial v}{\partial z} - \frac{v}{r}, \gamma_{xz} = \frac{\partial w}{\partial x} + \frac{\partial u}{\partial z}, \\ &\gamma_{x\theta} = \frac{\partial v}{\partial x} + \frac{1}{r}\frac{\partial u}{\partial \theta}, \end{aligned} \quad (3)$$

Using Eq. (1) and substitution into Eq. (3), the strain components are derived as follows:

$$\begin{aligned} \varepsilon_x &= \frac{\partial u_0}{\partial x} - z\frac{\partial^2 w_b}{\partial x^2} - f(z)\frac{\partial^2 w_s}{\partial x^2}, \\ \varepsilon_\theta &= \frac{1}{r}\left(1+\frac{z}{R}\right)\frac{\partial v_0}{\partial \theta} + \frac{w_b}{r} - \frac{z}{r^2}\frac{\partial^2 w_b}{\partial \theta^2} + \frac{w_s}{r} - \frac{f(z)}{r^2}\frac{\partial^2 w_s}{\partial \theta^2} + \frac{g(z)}{r}\chi, \\ \varepsilon_z &= g'(z)\chi, \\ \gamma_{x\theta} &= \left(1+\frac{z}{R}\right)\frac{\partial v_0}{\partial x} + \frac{1}{r}\frac{\partial u_0}{\partial \theta} - 2\frac{z}{r}\frac{\partial^2 w_b}{\partial x \partial \theta} - 2\frac{f(z)}{r}\frac{\partial^2 w_s}{\partial x \partial \theta}, \\ \gamma_{z\theta} &= \frac{2z}{r^2}\frac{\partial w_b}{\partial \theta} + \frac{1}{r}g(z)\frac{\partial w_s}{\partial \theta} - \left(\frac{z}{R}\right)\frac{v_0}{r} + \frac{g(z)}{r}\frac{\partial \chi}{\partial \theta}, \\ \gamma_{xz} &= g(z)\left(\frac{\partial w_s}{\partial x} + \frac{\partial \chi}{\partial x}\right), \end{aligned} \quad (4)$$

Based on Eq. (4), it is confirmed that one of out of plane shear strain is zero $\gamma_{xz}(z = \pm h/2) = g(z = \pm h/2)\left(\frac{\partial w_s}{\partial x} + \frac{\partial \chi}{\partial x}\right) = 0$ and another is approximately zero because of existence of terms r^2 and R in denominator.

The nano panel is subjected to electromagnetic loads, in which the electromagnetic fields are obtained as (Arefi and Zenkour 2017, 2018a, b):

$$\begin{aligned} \mathrm{E}_x &= \frac{\partial \Psi}{\partial x} cos\frac{\pi z}{h}, \mathrm{E}_\theta = \frac{1}{R+z}\frac{\partial \Psi}{\partial \theta} cos\frac{\pi z}{h}, \\ \mathrm{E}_z &= -\frac{2}{h}\Psi_0 - \frac{\pi}{h}\Psi sin\frac{\pi z}{h}, \\ \mathrm{H}_x &= \frac{\partial \Phi}{\partial x} cos\frac{\pi z}{h}, \mathrm{H}_\theta = \frac{1}{R+z}\frac{\partial \Phi}{\partial \theta} cos\frac{\pi z}{h}, \\ \mathrm{H}_z &= -\frac{2}{h}\Phi_0 - \frac{\pi}{h}\Phi sin\frac{\pi z}{h}, \end{aligned} \quad (5)$$

In which $\{\mathrm{E}_x, \mathrm{E}_\theta, \mathrm{E}_z\}$ electric field components and $\{\mathrm{H}_x, \mathrm{H}_\theta, \mathrm{H}_z\}$ magnetic field components. The nonlocal stress components are derived in electromagnetic environment as follow:

$$
\begin{aligned}
(1-\xi^2\nabla^2)\sigma_x &= C_{xxxx}\left\{\frac{\partial u_0}{\partial x}-z\frac{\partial^2 w_b}{\partial x^2}-f(z)\frac{\partial^2 w_s}{\partial x^2}\right\}\\
&+C_{xx\theta\theta}\left\{\frac{1}{r}\left(1+\frac{z}{R}\right)\frac{\partial v_0}{\partial\theta}+\frac{w_b}{r}-\frac{z}{r^2}\frac{\partial^2 w_b}{\partial\theta^2}+\frac{w_s}{r}-\frac{f(z)}{r^2}\frac{\partial^2 w_s}{\partial\theta^2}+\frac{g(z)\chi}{r}\right\}\\
&+C_{xxzz}\{g'(z)\chi\}-e_{xxz}\left\{-\frac{2}{h}\Psi_0-\frac{\pi}{h}\Psi sin\frac{\pi z}{h}\right\}-q_{xxz}\left\{-\frac{2}{h}\Phi_0-\frac{\pi}{h}\Phi sin\frac{\pi z}{h}\right\}\\
(1-\xi^2\nabla^2)\sigma_\theta &= C_{\theta\theta xx}\left\{\frac{\partial u_0}{\partial x}-z\frac{\partial^2 w_b}{\partial x^2}-f(z)\frac{\partial^2 w_s}{\partial x^2}\right\}\\
&+C_{\theta\theta\theta\theta}\left\{\frac{1}{r}\left(1+\frac{z}{R}\right)\frac{\partial v_0}{\partial\theta}+\frac{w_b}{r}-\frac{z}{r^2}\frac{\partial^2 w_b}{\partial\theta^2}+\frac{w_s}{r}-\frac{f(z)}{r^2}\frac{\partial^2 w_s}{\partial\theta^2}+\frac{g(z)\chi}{r}\right\}\\
&+C_{\theta\theta zz}\{g'(z)\chi\}-e_{\theta\theta z}\left\{-\frac{2}{h}\Psi_0-\frac{\pi}{h}\Psi sin\frac{\pi z}{h}\right\}-q_{\theta\theta z}\left\{-\frac{2}{h}\Phi_0-\frac{\pi}{h}\Phi sin\frac{\pi z}{h}\right\}\\
(1-\xi^2\nabla^2)\sigma_z &= C_{zzxx}\left\{\frac{\partial u_0}{\partial x}-z\frac{\partial^2 w_b}{\partial x^2}-f(z)\frac{\partial^2 w_s}{\partial x^2}\right\}\\
&+C_{zz\theta\theta}\left\{\frac{1}{r}\left(1+\frac{z}{R}\right)\frac{\partial v_0}{\partial\theta}+\frac{w_b}{r}-\frac{z}{r^2}\frac{\partial^2 w_b}{\partial\theta^2}+\frac{w_s}{r}-\frac{f(z)}{r^2}\frac{\partial^2 w_s}{\partial\theta^2}+\frac{g(z)\chi}{r}\right\}\\
&+C_{zzzz}\{g'(z)\chi\}-e_{zzz}\left\{-\frac{2}{h}\Psi_0-\frac{\pi}{h}\Psi sin\frac{\pi z}{h}\right\}-q_{xxz}\left\{-\frac{2}{h}\Phi_0-\frac{\pi}{h}\Phi sin\frac{\pi z}{h}\right\}\\
(1-\xi^2\nabla^2)\tau_{x\theta} &= C_{x\theta x\theta}\left\{\left(1+\frac{z}{R}\right)\frac{\partial v_0}{\partial x}+\frac{1}{r}\frac{\partial u_0}{\partial\theta}-2\frac{z}{r}\frac{\partial^2 w_b}{\partial x\partial\theta}-2\frac{f(z)}{r}\frac{\partial^2 w_s}{\partial x\partial\theta}\right\},\\
(1-\xi^2\nabla^2)\tau_{\theta z} &= C_{\theta z\theta z}\left\{\frac{2z}{r^2}\frac{\partial w_b}{\partial\theta}+\frac{1}{r}g(z)\frac{\partial w_s}{\partial\theta}-\left(\frac{z}{R}\right)\frac{v_0}{r}+\frac{g(z)}{r}\frac{\partial\chi}{\partial\theta}\right\}-e_{\theta zx}\left\{\frac{1}{r}\frac{\partial\Psi}{\partial\theta}cos\frac{\pi z}{h}\right\}-q_{\theta zx}\left\{\frac{1}{r}\frac{\partial\Phi}{\partial\theta}cos\frac{\pi z}{h}\right\},\\
(1-\xi^2\nabla^2)\tau_{xz} &= C_{xzxz}\left\{g(z)\left(\frac{\partial w_s}{\partial x}+\frac{\partial\chi}{\partial x}\right)\right\}-e_{xzx}\left\{\frac{\partial\Psi}{\partial x}cos\frac{\pi z}{h}\right\}-q_{xzx}\left\{\frac{\partial\Phi}{\partial x}cos\frac{\pi z}{h}\right\},
\end{aligned}
\tag{6}
$$

where, C_{ijkl} are stiffness coefficients, e_{ij} are piezoelectric coefficients, q_{ij} are piezomagnetic coefficients.

Furthermore, the electric displacements are obtained as:

$$
\begin{aligned}
(1-\xi^2\nabla^2)D_x &= e_{xxz}\left\{g(z)\left(\frac{\partial w_s}{\partial x}+\frac{\partial\chi}{\partial x}\right)\right\}+\eta_{xx}\left\{\frac{\partial\Psi}{\partial x}cos\frac{\pi z}{h}\right\}+d_{xx}\left\{\frac{\partial\Phi}{\partial x}cos\frac{\pi z}{h}\right\},\\
(1-\xi^2\nabla^2)D_\theta &= e_{\theta\theta z}\left\{\frac{2z}{r^2}\frac{\partial w_b}{\partial\theta}+\frac{1}{r}g(z)\frac{\partial w_s}{\partial\theta}-\left(\frac{z}{R}\right)\frac{v_0}{r}+\frac{g(z)}{r}\frac{\partial\chi}{\partial\theta}\right\}+\eta_{\theta\theta}\left\{\frac{1}{r}\frac{\partial\Psi}{\partial\theta}cos\frac{\pi z}{h}\right\}+d_{\theta\theta}\left\{\frac{1}{r}\frac{\partial\Phi}{\partial\theta}cos\frac{\pi z}{h}\right\},\\
(1-\xi^2\nabla^2)D_z &= e_{zxx}\left\{\frac{\partial u_0}{\partial x}-z\frac{\partial^2 w_b}{\partial x^2}-f(z)\frac{\partial^2 w_s}{\partial x^2}\right\}\\
&+e_{z\theta\theta}\left\{\frac{1}{r}\left(1+\frac{z}{R}\right)\frac{\partial v_0}{\partial\theta}+\frac{w_b}{r}-\frac{z}{r^2}\frac{\partial^2 w_b}{\partial\theta^2}+\frac{w_s}{r}-\frac{f(z)}{r^2}\frac{\partial^2 w_s}{\partial\theta^2}+\frac{g(z)\chi}{r}\right\}\\
&+e_{zzz}\{g'(z)\chi\}+\eta_{zz}\left\{-\frac{2}{h}\Psi_0-\frac{\pi}{h}\Psi sin\frac{\pi z}{h}\right\}+d_{zz}\left\{-\frac{2}{h}\Phi_0-\frac{\pi}{h}\Phi sin\frac{\pi z}{h}\right\},
\end{aligned}
\tag{7}
$$

In which, η_{ij} and d_{ij} are dielectric are magnetoelectric coefficients, respectively.

The magnetic induction relations are developed as:

$$
\begin{aligned}
(1-\xi^2\nabla^2)B_x &= q_{xxz}\left\{g(z)\left(\frac{\partial w_s}{\partial x}+\frac{\partial\chi}{\partial x}\right)\right\}+d_{xx}\left\{\frac{\partial\Psi}{\partial x}cos\frac{\pi z}{h}\right\}+\mu_{xx}\left\{\frac{\partial\Phi}{\partial x}cos\frac{\pi z}{h}\right\},\\
(1-\xi^2\nabla^2)B_\theta &= q_{\theta\theta z}\left\{\frac{2z}{r^2}\frac{\partial w_b}{\partial\theta}+\frac{1}{r}g(z)\frac{\partial w_s}{\partial\theta}-\left(\frac{z}{R}\right)\frac{v_0}{r}+\frac{g(z)}{r}\frac{\partial\chi}{\partial\theta}\right\}+d_{\theta\theta}\left\{\frac{1}{r}\frac{\partial\Psi}{\partial\theta}cos\frac{\pi z}{h}\right\}+\mu_{\theta\theta}\left\{\frac{1}{r}\frac{\partial\Phi}{\partial\theta}cos\frac{\pi z}{h}\right\},\\
(1-\xi^2\nabla^2)B_z &= q_{zxx}\left\{\frac{\partial u_0}{\partial x}-z\frac{\partial^2 w_b}{\partial x^2}-f(z)\frac{\partial^2 w_s}{\partial x^2}\right\}\\
&+q_{z\theta\theta}\left\{\frac{1}{r}\left(1+\frac{z}{R}\right)\frac{\partial v_0}{\partial\theta}+\frac{w_b}{r}-\frac{z}{r^2}\frac{\partial^2 w_b}{\partial\theta^2}+\frac{w_s}{r}-\frac{f(z)}{r^2}\frac{\partial^2 w_s}{\partial\theta^2}+\frac{g(z)\chi}{r}\right\}\\
&+q_{zzz}\{g'(z)\chi\}+d_{zz}\left\{-\frac{2}{h}\Psi_0-\frac{\pi}{h}\Psi sin\frac{\pi z}{h}\right\}+\mu_{zz}\left\{-\frac{2}{h}\Phi_0-\frac{\pi}{h}\Phi sin\frac{\pi z}{h}\right\},
\end{aligned}
\tag{8}
$$

where q_{ij} and μ_{ij} are piezomagnetic and magnetic coefficients.

Variation of strain energy is computed as follows (Mohammadimehr *et al.* 2016, Arefi *et al.* 2011, 2012,

2013, 2016a, b, Arefi and Rahimi 2011a, b, 2012a, b, Arefi and Zenkour 2018a, b, Arefi and Rabczuk 2019, Arefi 2013, 2014):

$$\begin{aligned} U=\int_{\theta}\int_{x}\Bigg(&\left\{N_x\frac{\partial\delta u_0}{\partial x}-M_x\frac{\partial^2\delta w_b}{\partial x^2}-S_x\frac{\partial^2\delta w_s}{\partial x^2}\right\}+\left\{P_\theta\frac{\partial\delta v_0}{\partial\theta}+N_\theta\delta w_b-M_\theta\frac{\partial^2\delta w_b}{\partial\theta^2}+G_\theta\delta w_s-S_\theta\frac{\partial^2\delta w_s}{\partial\theta^2}+Q_\theta\delta\chi\right\}+\{N_z\delta\chi\}\\ &+\left\{N_{x\theta}\frac{\partial\delta v_0}{\partial x}+P_{x\theta}\frac{\partial\delta u_0}{\partial\theta}-M_{x\theta}\frac{\partial^2\delta w_b}{\partial x\partial\theta}-S_{x\theta}\frac{\partial^2\delta w_s}{\partial x\partial\theta}\right\}+\left\{M_{z\theta}\frac{\partial\delta w_b}{\partial\theta}+Q_{z\theta}\frac{\partial\delta w_s}{\partial\theta}-N_{z\theta}\delta v_0+Q_{z\theta}\frac{\partial\delta\chi}{\partial\theta}\right\}\\ &+\left\{Q_{xz}\frac{\partial\delta w_s}{\partial x}+Q_{xz}\frac{\partial\delta\chi}{\partial x}\right\}-\bar{D}_x\frac{\partial\delta\Psi}{\partial x}-\bar{D}_\theta\frac{\partial\delta\Psi}{\partial\theta}+\bar{D}_z\delta\Psi-\bar{B}_x\frac{\partial\delta\Phi}{\partial x}-\bar{B}_\theta\frac{\partial\delta\Phi}{\partial\theta}+B_z\delta\Phi\Bigg)d\theta dx, \end{aligned} \tag{9}$$

where, the mechanical, electrical and magnetic resultant components are defined as:

$$\begin{aligned} \{N_x,M_x,S_x\}&=\int_{-\frac{h}{2}}^{\frac{h}{2}}(R+z)\sigma_x\{1,z,f(z)\}\mathrm{d}z,\\ \{N_\theta,P_\theta,M_\theta,G_\theta,S_\theta,Q_\theta\}&=\int_{-\frac{h}{2}}^{\frac{h}{2}}\sigma_\theta(R+z)\left\{\frac{1}{r},\frac{1}{r}\left(1+\frac{z}{R}\right),\frac{z}{r^2},\frac{1}{r},\frac{f(z)}{r^2},\frac{g(z)}{r}\right\}\mathrm{d}z,\\ \{N_z\}&=\int_{-\frac{h}{2}}^{\frac{h}{2}}(R+z)g'(z)\sigma_z\mathrm{d}z,\\ \{N_{x\theta},P_{x\theta},M_{x\theta},S_{x\theta}\}&=\int_{-\frac{h}{2}}^{\frac{h}{2}}\tau_{x\theta}(R+z)\left\{\left(1+\frac{z}{R}\right),\frac{1}{r},2\frac{z}{r},2\frac{f(z)}{r}\right\}\mathrm{d}z,\\ \{M_{z\theta},Q_{z\theta},N_{z\theta},Q_{z\theta}\}&=\int_{-\frac{h}{2}}^{\frac{h}{2}}\tau_{x\theta}(R+z)\left\{\frac{2z}{r^2},\frac{g(z)}{r},\frac{z}{Rr},\frac{g(z)}{r}\right\}\mathrm{d}z,\\ \{Q_{xz}\}&=\int_{-\frac{h}{2}}^{\frac{h}{2}}(R+z)g(z)\tau_{xz}\mathrm{d}z,\\ \{\bar{D}_x,\bar{D}_\theta,\bar{D}_z\}&=\int_{-\frac{h}{2}}^{\frac{h}{2}}\left\{D_x(R+z)cos\frac{\pi z}{h},D_\theta cos\frac{\pi z}{h},D_z\frac{\pi}{h}(R+z)sin\frac{\pi z}{h}\right\}\mathrm{d}z\\ \{\bar{B}_x,\bar{B}_\theta,\bar{B}_z\}&=\int_{-\frac{h}{2}}^{\frac{h}{2}}\left\{B_x(R+z)cos\frac{\pi z}{h},B_\theta cos\frac{\pi z}{h},B_z\frac{\pi}{h}(R+z)sin\frac{\pi z}{h}\right\}\mathrm{d}z \end{aligned} \tag{10}$$

Arranging the variables after integration by part leads to:

$$\delta U=\int_{\theta}\int_{x}\begin{pmatrix} -\left[\frac{\partial N_x}{\partial x}+\frac{\partial P_{x\theta}}{\partial\theta}\right]\delta u_0-\left[\frac{\partial N_{x\theta}}{\partial x}+N_{z\theta}+\frac{\partial P_\theta}{\partial\theta}\right]\delta v_0+\left[N_\theta-\frac{\partial^2M_x}{\partial x^2}-\frac{\partial^2M_{x\theta}}{\partial x\partial\theta}-\frac{\partial M_{z\theta}}{\partial\theta}-\frac{\partial^2M_\theta}{\partial\theta^2}\right]\delta w_b\\ +\left[G_\theta-\frac{\partial^2S_x}{\partial x^2}-\frac{\partial^2S_{x\theta}}{\partial x\partial\theta}-\frac{\partial Q_{z\theta}}{\partial\theta}-\frac{\partial^2S_\theta}{\partial\theta^2}-\frac{\partial Q_{xz}}{\partial x}\right]\delta w_s+\left[Q_\theta+N_z-\frac{\partial Q_{z\theta}}{\partial\theta}-\frac{\partial Q_{xz}}{\partial x}\right]\delta\chi\\ +\left[\frac{\partial\bar{D}_x}{\partial x}+\frac{\partial\bar{D}_\theta}{\partial\theta}+\bar{D}_z\right]\delta\Psi+\left[\frac{\partial\bar{B}_x}{\partial x}+\frac{\partial\bar{B}_\theta}{\partial\theta}+B_z\right]\delta\Phi \end{pmatrix}d\theta dx \tag{11}$$

The variation of external work is obtained as:

$$\delta W=\int_0^l\left[P_i\left(\delta w_b+\delta w_s+g(z=-\frac{h}{2})\delta\chi\right)-F_f\left(\delta w_b+\delta w_s+g(z=+\frac{h}{2})\delta\chi\right)\right](R+z)d\theta dx, \tag{12}$$

where $F_f=K_1w_0-K_2\nabla^2w_0$. Applying the minimum total energy principle as $\delta\Pi=0$ in which $\Pi=-U+W$, gives final governing equations as follows:

$$\begin{aligned} &\delta u_0:\frac{\partial N_x}{\partial x}+\frac{\partial P_{x\theta}}{\partial\theta}=0,\qquad \delta v_0:\frac{\partial N_{x\theta}}{\partial x}+N_{z\theta}+\frac{\partial P_\theta}{\partial\theta}=0,\qquad \delta w_b:N_\theta-\frac{\partial^2M_x}{\partial x^2}-\frac{\partial^2M_{x\theta}}{\partial x\partial\theta}-\frac{\partial M_{z\theta}}{\partial\theta}-\frac{\partial^2M_\theta}{\partial\theta^2}=P_i-F_f,\\ &\delta\chi:Q_\theta+N_z-\frac{\partial Q_{z\theta}}{\partial\theta}-\frac{\partial Q_{xz}}{\partial x}=P_ig(z=-\frac{h}{2})-F_fg(z=+\frac{h}{2}), \end{aligned} \tag{13}$$

$$\delta\Psi: \frac{\partial \bar{D}_x}{\partial x} + \frac{\partial \bar{D}_\theta}{\partial \theta} + \bar{D}_z = 0, \qquad \delta\Phi: \frac{\partial \bar{B}_x}{\partial x} + \frac{\partial \bar{B}_\theta}{\partial \theta} + B_z = 0, \tag{13}$$

Finally, we will have:

$$\begin{aligned}
&\delta u_0: \aleph_1 \frac{\partial^2 u_0}{\partial x^2} + \aleph_{94} \frac{\partial^2 u_0}{\partial \theta^2} + (\aleph_4 + \aleph_{93}) \frac{\partial^2 v_0}{\partial x\, \partial \theta} - \aleph_2 \frac{\partial^3 w_b}{\partial x^3} - (\aleph_6 + \aleph_{95}) \frac{\partial^3 w_b}{\partial x \partial \theta^2} + \aleph_5 \frac{\partial w_b}{\partial x} \\
&- \aleph_3 \frac{\partial^3 w_s}{\partial x^3} - (\aleph_7 + \aleph_{96}) \frac{\partial^3 w_s}{\partial x \partial \theta^2} + \aleph_5 \frac{\partial w_s}{\partial x} + (\aleph_8 + \aleph_9) \frac{\partial \chi}{\partial x} + \aleph_{10} \frac{\partial \Psi}{\partial x} + \aleph_{11} \frac{\partial \Phi}{\partial x} + \frac{\partial N_{\Psi_0}}{\partial x} + \frac{\partial N_{\Phi_0}}{\partial x} = 0, \\
&\delta v_0: (\aleph_{168} + \aleph_{90}) \frac{\partial^2 u_0}{\partial x\, \partial \theta} + \aleph_{89} \frac{\partial^2 v_0}{\partial x^2} + \aleph_{171} \frac{\partial^2 v_0}{\partial \theta^2} - \aleph_{119} v_0 - \aleph_{173} \frac{\partial^3 w_b}{\partial \theta^3} - (\aleph_{169} + \aleph_{91}) \frac{\partial^3 w_b}{\partial \theta \partial x^2} + (\aleph_{117} + \aleph_{172}) \frac{\partial w_b}{\partial \theta} \\
&- \aleph_{174} \frac{\partial^3 w_s}{\partial \theta^3} - (\aleph_{170} + \aleph_{92}) \frac{\partial^3 w_s}{\partial \theta \partial x^2} + (\aleph_{118} + \aleph_{172}) \frac{\partial w_s}{\partial \theta} + (\aleph_{175} + \aleph_{120} + \aleph_{176}) \frac{\partial \chi}{\partial \theta} \\
&+ (\aleph_{177} - \aleph_{121}) \frac{\partial \Psi}{\partial \theta} + (\aleph_{178} - \aleph_{122}) \frac{\partial \Phi}{\partial \theta} + \frac{\partial P_{\theta,\Psi_0}}{\partial \theta} + \frac{\partial P_{\theta,\Phi_0}}{\partial \theta} = 0, \\
&\delta w_b: -\aleph_{12} \frac{\partial^3 u_0}{\partial x^3} - (\aleph_{98} + \aleph_{45}) \frac{\partial^3 u_0}{\partial \theta^2\, \partial x} + \aleph_{34} \frac{\partial u_0}{\partial x} - \aleph_{48} \frac{\partial^3 v_0}{\partial \theta^3} - (\aleph_{15} + \aleph_{97}) \frac{\partial^3 v_0}{\partial x^2\, \partial \theta} + (\aleph_{37} + \aleph_{107}) \frac{\partial v_0}{\partial \theta} \\
&+ \aleph_{13} \frac{\partial^4 w_b}{\partial x^4} + \aleph_{50} \frac{\partial^4 w_b}{\partial \theta^4} + (\aleph_{17} + \aleph_{99} + \aleph_{46}) \frac{\partial^4 w_b}{\partial x^2 \partial \theta^2} - (\aleph_{35} + \aleph_{16}) \frac{\partial^2 w_b}{\partial x^2} - (\aleph_{39} + \aleph_{49} + \aleph_{105}) \frac{\partial^2 w_b}{\partial \theta^2} + \aleph_{38} w_b \\
&+ \aleph_{14} \frac{\partial^4 w_s}{\partial x^4} + \aleph_{51} \frac{\partial^4 w_s}{\partial \theta^4} + (\aleph_{18} + \aleph_{100} + \aleph_{47}) \frac{\partial^4 w_s}{\partial x^2 \partial \theta^2} - (\aleph_{36} + \aleph_{16}) \frac{\partial^2 w_s}{\partial x^2} - (\aleph_{40} + \aleph_{106} + \aleph_{49}) \frac{\partial^2 w_s}{\partial \theta^2} + \aleph_{38} w_s \\
&- (\aleph_{19} + \aleph_{20}) \frac{\partial^2 \chi}{\partial x^2} - (\aleph_{52} + \aleph_{53} + \aleph_{108}) \frac{\partial^2 \chi}{\partial \theta^2} + (\aleph_{41} + \aleph_{42}) \chi - \aleph_{21} \frac{\partial^2 \Psi}{\partial x^2} + (\aleph_{109} - \aleph_{54}) \frac{\partial^2 \Psi}{\partial \theta^2} + \aleph_{43} \Psi \\
&- \aleph_{22} \frac{\partial^2 \Phi}{\partial x^2} + (\aleph_{110} - \aleph_{55}) \frac{\partial^2 \Phi}{\partial \theta^2} + \aleph_{44} \Phi - \frac{\partial^2 M_{\Psi_0}}{\partial x^2} - \frac{\partial^2 M_{\Phi_0}}{\partial x^2} - \frac{\partial^2 M_{\theta,\Psi_0}}{\partial \theta^2} - \frac{\partial^2 M_{\theta,\Phi_0}}{\partial \theta^2} + N_{\theta,\Psi_0} + N_{\theta,\Phi_0} = P_i - F_f,
\end{aligned}$$

$$\begin{aligned}
&\delta w_s: -\aleph_{23} \frac{\partial^3 u_0}{\partial x^3} - \aleph_{102} \frac{\partial^3 u_0}{\partial \theta^2\, \partial x} - \aleph_{56} \frac{\partial^3 u_0}{\partial \theta^2\, \partial x} + \aleph_{34} \frac{\partial u_0}{\partial x} - \aleph_{59} \frac{\partial^3 v_0}{\partial \theta^3} - (\aleph_{26} + \aleph_{101}) \frac{\partial^3 v_0}{\partial x^2\, \partial \theta} + (\aleph_{37} + \aleph_{113}) \frac{\partial v_0}{\partial \theta} \\
&+ \aleph_{24} \frac{\partial^4 w_b}{\partial x^4} + \aleph_{61} \frac{\partial^4 w_b}{\partial \theta^4} + \left(\aleph_{28} + \aleph_{103} + \aleph_{57} \frac{\partial^4 w_b}{\partial x^2 \partial \theta^2} \right) \frac{\partial^4 w_b}{\partial x^2 \partial \theta^2} - (\aleph_{27} + \aleph_{35}) \frac{\partial^2 w_b}{\partial x^2} - (\aleph_{39} + \aleph_{60} + \aleph_{111}) \frac{\partial^2 w_b}{\partial \theta^2} + \aleph_{38} w_b \\
&+ \aleph_{25} \frac{\partial^4 w_s}{\partial x^4} + \aleph_{62} \frac{\partial^4 w_s}{\partial \theta^4} + (\aleph_{29} + \aleph_{104} + \aleph_{58}) \frac{\partial^4 w_s}{\partial x^2 \partial \theta^2} - (\aleph_{27} + \aleph_{36} + \aleph_{123}) \frac{\partial^2 w_s}{\partial x^2} - (\aleph_{40} + \aleph_{60} + \aleph_{112}) \frac{\partial^2 w_s}{\partial \theta^2} + \aleph_{38} w_s \\
&- (\aleph_{30} + \aleph_{31} + \aleph_{123}) \frac{\partial^2 \chi}{\partial x^2} - (\aleph_{63} + \aleph_{64} + \aleph_{114}) \frac{\partial^2 \chi}{\partial \theta^2} + (\aleph_{41} + \aleph_{42}) \chi + (\aleph_{124} - \aleph_{32}) \frac{\partial^2 \Psi}{\partial x^2} + (\aleph_{115} - \aleph_{65}) \frac{\partial^2 \Psi}{\partial \theta^2} + \aleph_{43} \Psi \\
&+ (\aleph_{125} - \aleph_{33}) \frac{\partial^2 \Phi}{\partial x^2} + (\aleph_{116} - \aleph_{66}) \frac{\partial^2 \Phi}{\partial \theta^2} + \aleph_{44} \Phi - \frac{\partial^2 S_{\theta,\Psi_0}}{\partial \theta^2} - \frac{\partial^2 S_{\theta,\Phi_0}}{\partial \theta^2} - \frac{\partial^2 S_{\Psi_0}}{\partial x^2} - \frac{\partial^2 S_{\Phi_0}}{\partial x^2} + N_{\theta,\Psi_0} + N_{\theta,\Phi_0} = P_i - F_f,
\end{aligned} \tag{14}$$

$$\begin{aligned}
&\delta \chi: (\aleph_{67} + \aleph_{78}) \frac{\partial u_0}{\partial x} + (\aleph_{81} + \aleph_{113} + \aleph_{70}) \frac{\partial v_0}{\partial \theta} - (\aleph_{68} + \aleph_{79}) \frac{\partial^2 w_b}{\partial x^2} - (\aleph_{111} + \aleph_{83} + \aleph_{72}) \frac{\partial^2 w_b}{\partial \theta^2} + (\aleph_{71} + \aleph_{82}) w_b \\
&- (\aleph_{73} + \aleph_{84} + \aleph_{112}) \frac{\partial^2 w_s}{\partial \theta^2} - (\aleph_{69} + \aleph_{123} + \aleph_{80}) \frac{\partial^2 w_s}{\partial x^2} + (\aleph_{71} + \aleph_{82}) w_s - \aleph_{123} \frac{\partial^2 \chi}{\partial x^2} - \aleph_{114} \frac{\partial^2 \chi}{\partial \theta^2} \\
&+ (\aleph_{74} + \aleph_{75} + \aleph_{85} + \aleph_{86}) \chi + \aleph_{124} \frac{\partial^2 \Psi}{\partial x^2} + \aleph_{115} \frac{\partial^2 \Psi}{\partial \theta^2} + (\aleph_{87} + \aleph_{76}) \Psi + \aleph_{125} \frac{\partial^2 \Phi}{\partial x^2} + \aleph_{116} \frac{\partial^2 \Phi}{\partial \theta^2} \\
&+ (\aleph_{77} + \aleph_{88}) \Phi + N_{z,\Psi_0} + N_{z,\Phi_0} + Q_{\theta,\Psi_0} + Q_{\theta,\Phi_0} = P_i g(z = -\frac{h}{2}) - F_f g(z = +\frac{h}{2}), \\
&\delta \Psi: +\aleph_{135} \frac{\partial u_0}{\partial x} + (\aleph_{138} - \aleph_{131}) \frac{\partial v_0}{\partial \theta} - \aleph_{136} \frac{\partial^2 w_b}{\partial x^2} + (\aleph_{129} - \aleph_{140}) \frac{\partial^2 w_b}{\partial \theta^2} + \aleph_{139} w_b + (\aleph_{126} - \aleph_{137}) \frac{\partial^2 w_s}{\partial x^2} \\
&+ (\aleph_{130} - \aleph_{142}) \frac{\partial^2 w_s}{\partial \theta^2} + \aleph_{141} w_s + \aleph_{126} \frac{\partial^2 \chi}{\partial x^2} + \aleph_{132} \frac{\partial^2 \chi}{\partial \theta^2} + (\aleph_{143} + \aleph_{144}) \chi \\
&+ \aleph_{127} \frac{\partial^2 \Psi}{\partial x^2} + \aleph_{133} \frac{\partial^2 \Psi}{\partial \theta^2} - \aleph_{145} \Psi + \aleph_{128} \frac{\partial^2 \Phi}{\partial x^2} + \aleph_{134} \frac{\partial^2 \Phi}{\partial \theta^2} - \aleph_{146} \Phi - D_{\Psi_0} - D_{\Phi_0} = 0, \\
&\delta \Phi: +\aleph_{156} \frac{\partial u_0}{\partial x} + (\aleph_{159} - \aleph_{152}) \frac{\partial v_0}{\partial \theta} - \aleph_{157} \frac{\partial^2 w_b}{\partial x^2} + (\aleph_{150} - \aleph_{161}) \frac{\partial^2 w_b}{\partial \theta^2} + \aleph_{160} w_b + \aleph_{151} \frac{\partial^2 w_s}{\partial \theta^2} + \\
&(\aleph_{147} - \aleph_{158}) \frac{\partial^2 w_s}{\partial x^2} - \aleph_{163} \frac{\partial^2 w_s}{\partial \theta^2} + \aleph_{162} w_s + \aleph_{147} \frac{\partial^2 \chi}{\partial x^2} + \aleph_{153} \frac{\partial^2 \chi}{\partial \theta^2} + (\aleph_{164} + \aleph_{165}) \chi \\
&+ \aleph_{154} \frac{\partial^2 \Psi}{\partial \theta^2} + \aleph_{148} \frac{\partial^2 \Psi}{\partial x^2} - \aleph_{166} \Psi + \aleph_{149} \frac{\partial^2 \Phi}{\partial x^2} + \aleph_{155} \frac{\partial^2 \Phi}{\partial \theta^2} - \aleph_{167} \Phi - B_{\Phi_0} - B_{\Psi_0} = 0,
\end{aligned}$$

3. Solution, numerical results and discussion

Numerical results are expressed in this section to investigate impact of main parameters such as initial electromagnetic potentials, nano scale parameter and length to radius ratio on the results. The unknown functions are assumed as:

$$\begin{Bmatrix} u_0 \\ v_0 \\ w_b \\ w_s \\ \chi \\ \Psi \\ \Phi \end{Bmatrix} = \sum_{m=1}^{\infty}\sum_{n=1}^{\infty} \begin{Bmatrix} U_{mn} cos\frac{n\pi x}{L} sin\frac{m\pi\theta}{\Theta} \\ V_{mn} sin\frac{n\pi x}{L} cos\frac{m\pi\theta}{\Theta} \\ W^b_{mn} sin\frac{n\pi x}{L} sin\frac{m\pi\theta}{\Theta} \\ W^s_{mn} sin\frac{n\pi x}{L} sin\frac{m\pi\theta}{\Theta} \\ \mathrm{X}_{mn} sin\frac{n\pi x}{L} sin\frac{m\pi\theta}{\Theta} \\ \Psi_{mn} sin\frac{n\pi x}{L} sin\frac{m\pi\theta}{\Theta} \\ \Phi_{mn} sin\frac{n\pi x}{L} sin\frac{m\pi\theta}{\Theta} \end{Bmatrix}, \quad (15)$$

$$\alpha_n = \frac{n\pi}{L}, \ \beta_m = \frac{m\pi}{\Theta}$$

where $U_{mn}, V_{mn}, W^b_{mn}, W^s_{mn}, \mathrm{X}_{mn}, \Psi_{mn}, \Phi_{mn}$ are maximum amplitudes of axial and circumferential displacements, bending, shear and stretching deflections, maximum electric and magnetic potentials, respectively.

Unknown displacement, rotation and electric/magnetic potentials are obtained using solution of Eq. (13) as:

$$[K]\{X\} = \{F\}, \quad (16)$$

The numerical results are presented in this section in terms of main parameters of the problem. The transverse loading is assumed sinusoidal. Based on this assumption, we will have:

$$P_i = \bar{\mathrm{P}}_i sin\frac{n\pi x}{L} sin\frac{m\pi\theta}{\Theta}, \qquad \mathrm{m} = \mathrm{n} = 1 \quad (17)$$

In which $\bar{\mathrm{P}}_i$ is maximum pressure at middle of cylindrical panel. To investigate effect of out of plane normal strain on the results, some figures are provided to present transverse displacement along the thickness direction based on various input parameters. Fig. 1 shows changes of dimensionless radial displacement $\bar{w}$ along the thickness direction in terms of various nano scale parameter $\bar{\xi}$. An important effect of thickness stretching on the transverse displacement is observed in this figure. An increase in transverse displacement is observed with increase in $\bar{\xi}$.

Figs. and, 3 show changes of $\bar{\chi}$ of piezomagnetic nano panel in terms of small scale parameter for various Ψ_0, Φ_0 respectively. A decrease in $\bar{\chi}$ is observed with an increase in Ψ_0, Φ_0. Furthermore, a significant increase in $\bar{\chi}$ is observed with an increase in nonlocal parameter because of a decrease in structural stiffness.

Shown in Figs. 4 and 5 are changes of $\bar{U}$ of piezo-magnetic nano panel in terms of various nano scale parameter $\bar{\xi}$ for various applied electromagnetic potentials Ψ_0, Φ_0 respectively. A decrease in dimensionless axial

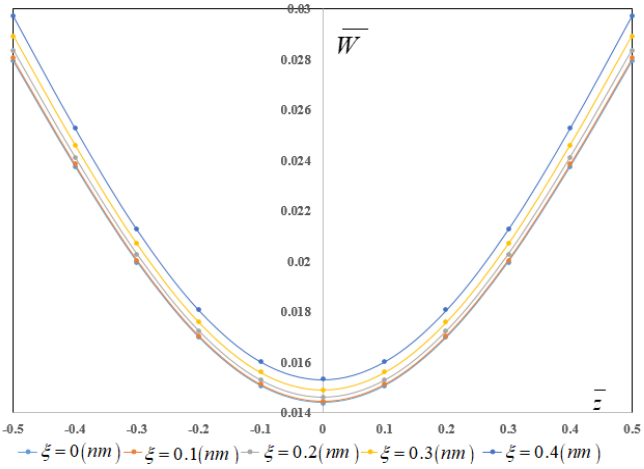

Fig. 1 Changes of $\bar{w}$ in terms of $\bar{z}$ for various $\bar{\xi}$

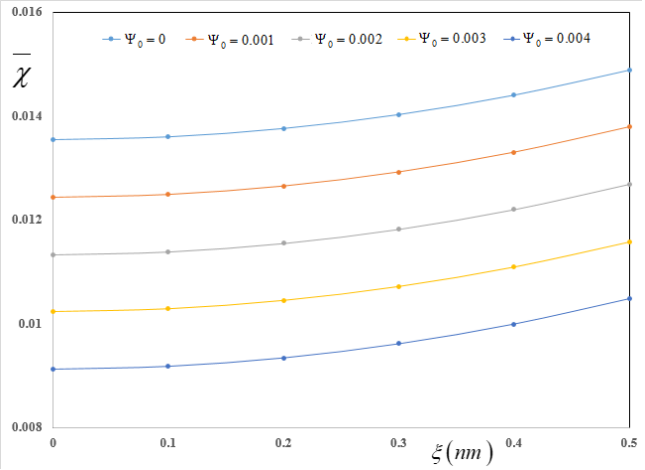

Fig. 2 Changes of $\bar{\chi}$ of in terms of small scale parameter for various Ψ_0

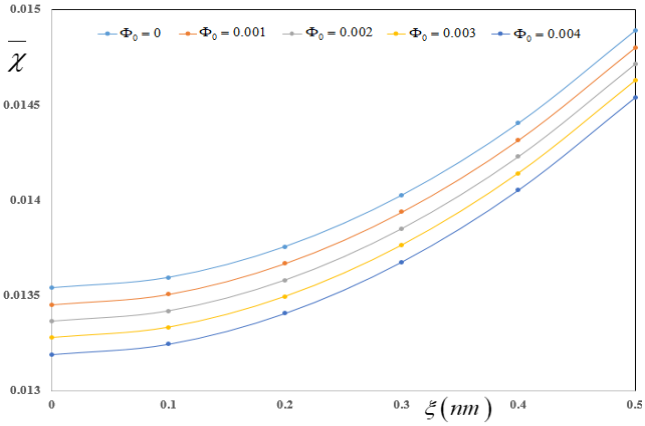

Fig. 3 Changes of $\bar{U}$ in terms of various $\bar{\xi}$ for various Φ_0

displacement $\bar{U}$ is observed with a decrease in Ψ_0 and an increase in Φ_0.

To investigate effect of initial electromagnetic loads as well as small scale parameter in nano scale on the bending deflection of piezomagnetic nano panel, Figs. 6 and 7 are produced. Figures 6 and 7 show changes of $\overline{W_b}$ in terms of small scale parameter in nano scale for various Ψ_0, Φ_0. It is

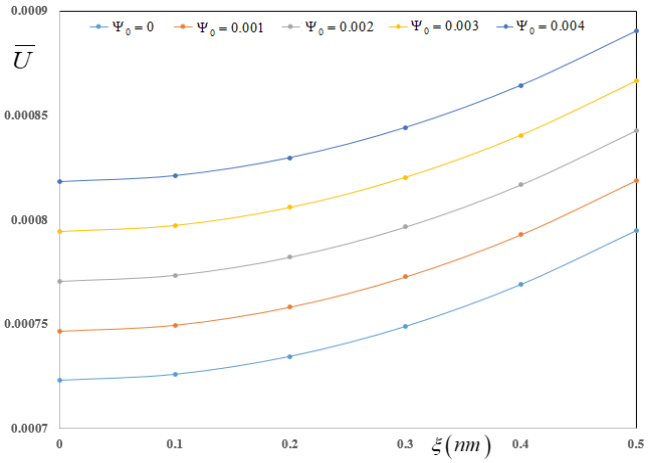

Fig. 4 Changes of $\overline{U}$ in terms of $\bar{\xi}$ for various Ψ_0

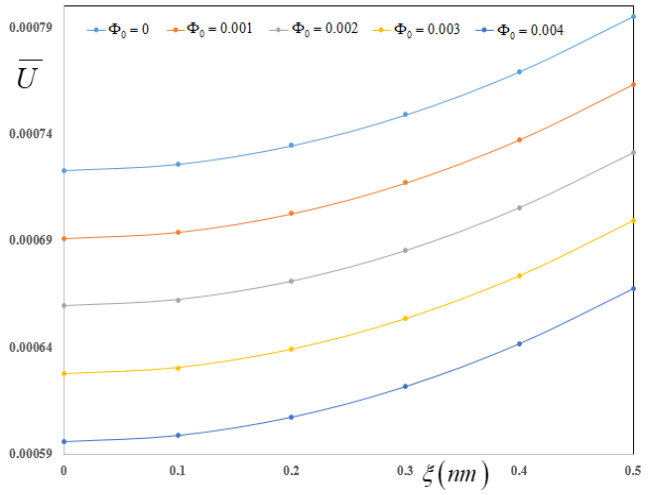

Fig. 5 Effect of various $\bar{\xi}$ and Ψ_0 on the $\bar{\phi}$

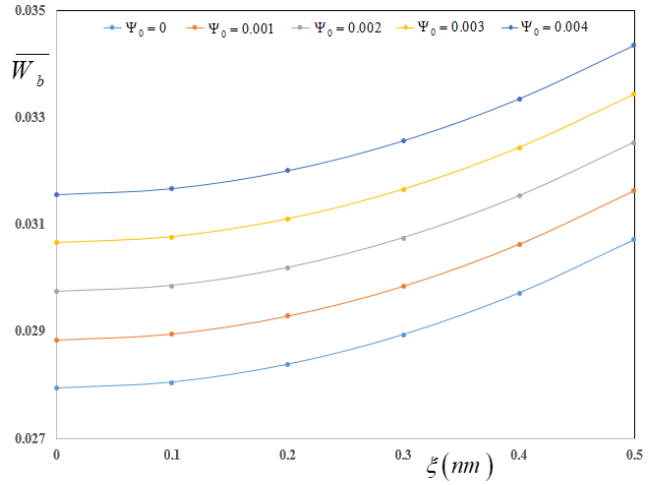

Fig. 6 Changes of $\overline{W_b}$ in terms of $\bar{\xi}$ for various Ψ_0

concluded that the bending deflection is increased with an increase in applied electric potential. Furthermore, a decrease in bending deflection is observed with an increase in applied magnetic potential.

Two-dimensional variation of $\bar{\chi}$ in terms of nonlocal parameter and span angle is presented in Fig. 8. An important

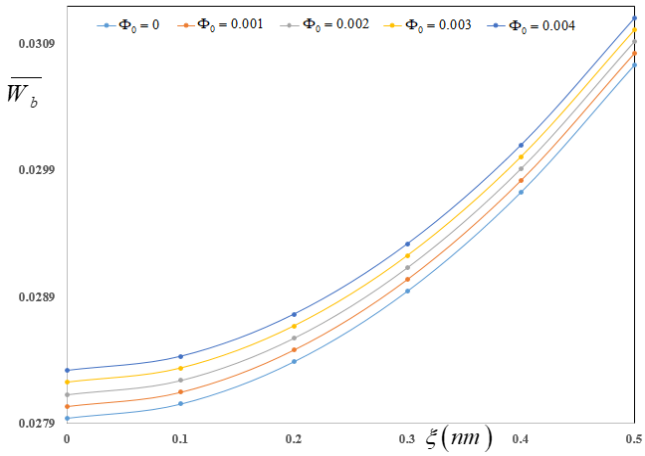

Fig. 7 Changes of $\overline{W_b}$ in terms of $\bar{\xi}$ for various Φ_0

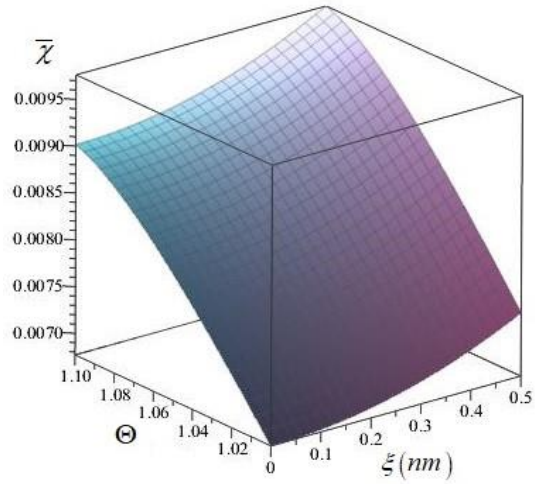

Fig. 8 Two-dimensional variation of $\bar{\chi}$ in terms of $\bar{\xi}$ and Θ

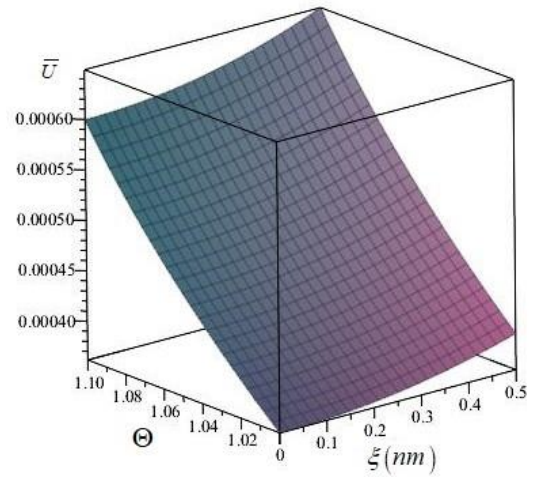

Fig. 9 Two-dimensional variation of $\overline{U}$ in terms of $\bar{\xi}$ and Θ

increase of $\bar{\chi}$ is concluded with increase in nonlocal parameter and span angle. Figs. 9 and 10 show changes of $\overline{U}$ $\overline{W_b}$ of piezomagnetic nano panel in terms of $\bar{\xi}$ and Θ, respectively. One can conclude that the both axial and

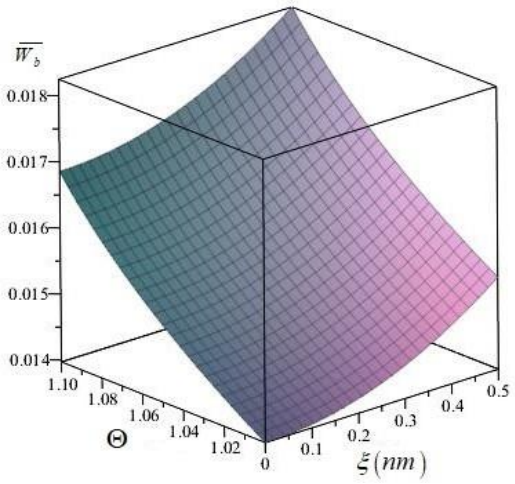

Fig. 10 Two-dimensional variation of $\overline{W_b}$ in terms of $\bar{\xi}$ and Θ

bending displacements are increased with increase of $\bar{\xi}$and Θ because of decrease of stiffness of nano panel. It is confirmed that with an increase in span angle, the structural stiffness is decreased and consequently the displacements are increased.

4. Conclusions

Electromagnetoelastic analysis of a cylindrical panel in electromagnetic environment was studied in this paper. The kinematic relations were developed based on HOSNDT to include out of plane normal strain in governing equations. The piezomagnetic nano panel was subjected to an initial electromagnetic loads and a two dimensional electromagnetic potentials along the axial and circumferential directions. An extended parametric results are presented for investigating impact of main inputs on the electromagnetoelastic results. The main numerical results of the present paper are expressed as:

Investigating effect of initial electromagnetic loads on the bending behavior of nano panel show that decrease in dimensionless axial displacement $\bar{U}$ is observed with decrease in applied electric potential Ψ_0 and increase in applied magnetic potential Φ_0.

Investigating effect of nonlocal parameter $\bar{\xi}$ and span angle Θ on the variation of axial $\bar{U}$ and bending deflection $\overline{W_b}$ of piezomagnetic nano panel show that both axial and bending displacements are increased with increase of nonlocal parameter and span angle because of decrease of stiffness of nano panel.

Increase in nonlocal parameter leads to increase in all displacements. As an important result, one can conclude that effect of small scale parameter is very important on the changes of thickness stretching displacement than the axial displacement.

Acknowledgments

This work was supported by Guangzhou City Philosophy and Social Science Planning Project “Guangzhou Speeds Up the Development of Artificial Intelligence and Digital Economy Pilot Zone Construction research” (Project No. 2021GZGJ24).

This work was supported by National Natural Science Foundation (51508261), the Doctoral Program of Shandong Jiaotong University.

References

Adim, B. and Daouadji, T.H. (2016), “Effects of thickness stretching in FGM plates using a quasi-3D higher order shear deformation theory”, *Adv. Mater. Res.*, **5**(4), 223-244. http://doi.org/10.12989/amr.2016.5.4.223.

Alijani, F. and Amabili, M. (2014a), “Effect of thickness deformation on large-amplitude vibrations of functionally graded rectangular plates”, *Compos. Struct.*, **113**, 89-107. https://doi.org/10.1016/j.compstruct.2014.03.006.

Alijani, F. and Amabili, M. (2014b), “Non-linear static bending and forced vibrations of rectangular plates retaining non-linearities in rotations and thickness deformation”, *Int. J. Non-Linear Mech.*, **67**, 394-404. https://doi.org/10.1016/j.ijnronlinmec.2014.10.003.

Amabili, M. (2014), “A non-linear higher-order thickness stretching and shear deformation theory for large-amplitude vibrations of laminated doubly curved shells”, *Int. J. Non-Linear Mech.*, **58**, 57-75. https://doi.org/10.1016/j.ijnonlinmec.2013.08.006.

Amabili, M. (2015), “Non-linearities in rotation and thickness deformation in a new third-order thickness deformation theory for static and dynamic analysis of isotropic and laminated doubly curved shells”, *Int. J. Non-Linear Mech.*, **69**, 109-128. https://doi.org/10.1016/j.ijnonlinmec.2014.11.026.

Amabili, M. and Reddy, J.N. (2020), “The nonlinear, third-order thickness and shear deformation theory for statics and dynamics of laminated composite shells”, *Compos. Struct.*, **244**, 112265. https://doi.org/10.1016/j.compstruct.2020.112265.

Arefi, M., Rahimi, G.H. and Khoshgoftar, M.J. (2011), “Optimized design of a cylinder under mechanical, magnetic and thermal loads as a sensor or actuator using a functionally graded piezomagnetic material”, *Int. J. Phys. Sci.*, **6**(27), 6315-6322. https://doi.org/10.5897/IJPS10.597.

Arefi, M. and Rahimi, G.H. (2011), “Thermo elastic analysis of a functionally graded cylinder under internal pressure using first order shear deformation theory”, *Sci. Res. Essays*, **5**(12), 1442-1454. https://doi.org/10.5897/SRE.9000953.

Arefi, M. and Rahimi, G.H. (2012a), “Studying the nonlinear behavior of the functionally graded annular plates with piezoelectric layers as a sensor and actuator under normal pressure”, *Smart. Struct. Syst.* **9**(2), 127-143. https://doi.org/10.12989/sss.2011.8.5.433.

Arefi, M. and Rahimi, G.H. (2012b), “Comprehensive thermoelastic analysis of a functionally graded cylinder with different boundary conditions under internal pressure using first order shear deformation theory”, *Mechanika*, **18**(1), 5-13. https://doi.org/10.5755/j01.mech.18.1.1273.

Arefi, M. and Rahimi, G.H. (2012c), “Non linear analysis of a functionally graded square plate with two smart layers as sensor and actuator under normal pressure”, *Smart. Struct. Syst.*, **8**(5), 433-447. https://doi.org/10.12989/sss.2011.8.5.433.

Arefi, M., Rahimi, G.H. and Khoshgoftar, M.J. (2012), “Exact solution of a thick walled functionally graded piezoelectric cylinder under mechanical, thermal and electrical loads in the magnetic field”, *Smart. Struct. Syst.*, **9**(5), 427-439. https://doi.org/10.12989/sss.2012.9.5.427.

Arefi, M. (2013), “Nonlinear thermoelastic analysis of thick-walled functionally graded piezoelectric cylinder”, *Acta Mechanica*, **224**(11), 2771-2783. https://doi.org/10.1007/s00707-013-0888-0.

Arefi, M. (2014), "A complete set of equations for piezo-magnetoelastic analysis of a functionally graded thick shell of revolution", *Lat. Amer. J. Solids. Struct.*, **11**, 2073-2092. https://doi.org/10.1590/S1679-78252014001100009.

Arefi, M., Karroubi, R. and Irani-Rahaghi, M. (2016a), "Free vibration analysis of functionally graded laminated sandwich cylindrical shells integrated with piezoelectric layer", *Appl. Math. Mech.* **37**(7), 821-834. https://doi.org/10.1007/s10483-016-2098-9.

Arefi, M., Karroubi, R. and Irani-Rahaghi, M. (2016b), "Free vibration analysis of functionally graded laminated sandwich cylindrical shells integrated with piezoelectric layer", *Appl. Math. Mech.*, **37**(7), 821-834. https://doi.org/10.1007/s10483-016-2098-9.

Arefi, M. and Zenkour, A.M. (2017), "Transient analysis of a three-layer microbeam subjected to electric potential", *Int. J. Smart. Nano. Mater.*, **8**(1), 20-40. https://doi.org/10.1080/19475411.2017.1292967.

Arefi, M. and Zenkour, A.M. (2018a), "Size-dependent electro-elastic analysis of a sandwich microbeam based on higher-order sinusoidal shear deformation theory and strain gradient theory", *J. Intel. Mater. Syst. Struct.*, **29** (7), 1394-1406. https://doi.org/10.1177/1045389X17733333.

Arefi, M. and Zenkour, A.M. (2018b), "Size-dependent electro-elastic analysis of a sandwich microbeam based on higher-order sinusoidal shear deformation theory and strain gradient theory", *J. Intel. Mater. Syst. Struct.*, **29**(7), 1394-1406. https://doi.org/10.1177/1045389X17733333.

Arefi, M. and Rabczuk, T. (2019), "A nonlocal higher order shear deformation theory for electro-elastic analysis of a piezoelectric doubly curved nano shell", *Compos. B: Eng.*, **168**(1), 496-510. https://doi.org/10.1016/j.compositesb.2019.03.065.

Asrari, R., Ebrahimi, F. and Kheirikhah, M.M. (2020), "On scale-dependent stability analysis of functionally graded magneto-electro-thermo-elastic cylindrical nanoshells", *Struct. Eng. Mech.*, **75**(6), 659-674. https://doi.org/10.12989/sem.2020.75.6.659.

Asghar, S., Naeem, M.N., Hussain, M. and Tounsi, A. (2020), "Nonlocal vibration of DWCNTs based on Flügge shell model using wave propagation approach", *Steel Compos. Struct.*, **34**(4), 599-613. https://doi.org/10.12989/scs.2020.34.4.599.

Asiri, S.A., Akbas, S.D. and Eltaher, M.A. (2020), "Damped dynamic responses of a layered functionally graded thick beam under a pulse load", *Struct. Eng. Mech.*, **75**(6), 713-722. https://doi.org/10.12989/sem.2020.75.6.713.

Alibeigloo, A. and Liew, K.M. (2014), "Free vibration analysis of sandwich cylindrical panel with functionally graded core using three-dimensional theory of elasticity", *Compos. Struct.*, **113**, 23-30. https://doi.org/10.1016/j.compstruct.2014.03.004.

Atmane, H.A. Tounsi, A. and Bernard, F. (2017), "Effect of thickness stretching and porosity on mechanical response of a functionally graded beams resting on elastic foundations", *Int. J. Mech. Mater. Design.*, **13**, 71-84. https://doi.org/10.1007/s10999-015-9318-x.

Barati, M.R. and Zenkour, A.M. (2019), "Vibration analysis of functionally graded graphene platelet reinforced cylindrical shells with different porosity distribution", *Mech. Adv. Mater. Struct.*, **26**(18), 1580-1588. https://doi.org/10.1080/15376494.2018.1444235.

Belarbi, M. Tati, A. and Khechai, A. (2019), "Effect of thickness stretching on the natural frequencies of laminate-faced sandwich plates using a new Layerwise model", *J. Build. Mater. Struct.* **6**, 88-96. https://doi.org/10.5281/zenodo.3352310.

Bellal, M., Hebali, H., Heireche, H., Bousahla, A.A., Tounsi, A., Bourada, F., Mahmoud, S.R., Bedia, E.A. and Tounsi, A. (2020), "Buckling behavior of a single-layered graphene sheet resting on viscoelastic medium via nonlocal four-unknown integral model", *Steel Compos. Struct.*, **34**(5), 643-655. https://doi.org/10.12989/scs.2020.34.5.643.

Bodaghi, M. and Shakeri, M. (2012), "An analytical approach for free vibration and transient response of functionally graded piezoelectric cylindrical panels subjected to impulsive loads", *Compos. Struct.* **94**, 1721-1735. https://doi.org/10.1016/j.compstruct.2012.01.009.

Carrera, E., Brischetto, S., Cinefra, M. and Soave, M. (2011), "Effects of thickness stretching in functionally graded plates and shells", *Compos. Part B. Eng.*, **42**(2), 123-133. https://doi.org/10.1016/j.compositesb.2010.10.005.

Chen, R., Cheng, Y., Wang, P., Wang, Q., Wan, S., Huang, S. and Wang, Y. (2021a). "Enhanced removal of Co(II) and Ni(II) from high-salinity aqueous solution using reductive self-assembly of three-dimensional magnetic fungal hyphal/graphene oxide nanofibers". *Sci. Total Environ.*, **756**, 143871. https://doi.org/10.1016/j.scitotenv.2020.143871.

Chen, R., Cheng, Y., Wang, P., Wang, Y., Wang, Q., Yang, Z. and Su, C. (2021b). "Facile synthesis of a sandwiched $Ti_3C_2T_x$ MXene/nZVI/fungal hypha nanofiber hybrid membrane for enhanced removal of Be(II) from $Be(NH_2)_2$ complexing solutions", *Chem. Eng. J.*, **421**, 129682. https://doi.org/10.1016/j.cej.2021.129682.

Elmascri, S., Bessaim, A., Taleb, O. Houari, M.S.A., Mohamed, S. Bernard, F. and Tounsi, A. (2020), "A novel hyperbolic plate theory including stretching effect for free vibration analysis of advanced composite plates in thermal environments, *Struct. Eng. Mech.*, **75**(2), 193-209, http://doi.org/10.12989/sem.2020.75.2.193.

Farrokhi Nia, A., Badnava, S., Hamouda, A.M.S., Mirjavadi, S.S. and Forsat, M. (2020), "Nonlocal strain gradient effects on forced vibrations of porous FG cylindrical nanoshells", *Adv. Nano. Res.*, **8**(2), 149-156. http://doi.org/10.12989/anr.2020.8.2.149.

Feng, S., Zuo, C., Zhang, L., Yin, W. and Chen, Q. (2021). "Generalized framework for non-sinusoidal fringe analysis using deep learning", *Photonic Res.*, **9**(6), 1084. https://doi.org/10.1364/PRJ.420944.

Gholami, Y., Ansari, R., Gholami, R. and Rouhi, H. (2020), "Nonlinear forced vibration analysis of FG cylindrical nanopanels based on Mindlin's strain gradient theory and 3D elasticity", *Int. J. Nonlinear. Sci. Num. Sim.*, **21**(6), 523-537. https://doi.org/10.1515/ijnsns-2018-0333.

Gupta, A., Talha, M. and Seemann, W. (2018), "Free vibration and flexural response of functionally graded plates resting on Winkler–Pasternak elastic foundations using nonpolynomial higher-order shear and normal deformation theory", *Mech. Adv. Mater. Struct.*, **25**(6), 523-538. https://doi.org/10.1080/15376494.2017.1285459.

Ganapathi, M., Anirudh, B., Anant, C. and Polit, O. (2019), "Dynamic characteristics of functionally graded graphene reinforced porous nanocomposite curved beams based on trigonometric shear deformation theory with thickness stretch effect", *Mech. Adv. Mater. Struct.*, **28**(7), 741-752. https://doi.org/10.1080/15376494.2019.1601310.

Guo, F., Wu, S., Liu, J., Wu, Z., Fu, S. and Ding, S. (2021). "A time-domain stepwise fatigue assessment to bridge small-scale fracture mechanics with large-scale system dynamics for high-speed maglev lightweight bogies". *Eng. Fract. Mech.*, **248**, 107711. https://doi.org/10.1016/j.engfracmech.2021.107711.

Hashemi, R., Mirzaei, M. and Adlparvar, M.R. (2021), "On thermally induced instability of FG-CNTRC cylindrical panels", *Adv. Nano. Res.*, **10**(1), 43-57. http://doi.org/10.12989/anr.2021.10.1.043.

Kabir, H.R.H. and Askar, H. (2005), "Free vibration response of cylindrical panels with higher order shear deformation theory", *Int. J. Struct. Stab. Dyn.*, **5**(3), 409-434. https://doi.org/10.1142/S0219455405001660.

Khoshgoftar, M.J., Rahimi, G.H. and Arefi, M. (2013), "Exact

solution of functionally graded thick cylinder with finite length under longitudinally non-uniform pressure", *Mech. Res. Com.* **51**, 61-66. https://doi.org/10.1016/j.mechrescom.2013.05.001.

Kheroubi, B., Benzair, A., Tounsi, A. and Semmah, A. (2016), "A new refined nonlocal beam theory accounting for effect of thickness stretching in nanoscale beams", *Adv. Nano. Res.*, **4**(4), 251-264. http://doi.org/10.12989/anr.2016.4.4.251.

Li, X., Dong, Z., Yu, P., Wang, L., Niu, X., Yamaguchi, H. and Li, D. (2021), "Effect of self-assembly on fluorescence in magnetic multiphase flows and its application on the novel detection for COVID-19". *Phys. Fluid.*, **33**(4). https://doi.org/10.1063/5.0048123.

Merzouki, T., Ganapathi, M. and Polit, O. (2019), "A nonlocal higher-order curved beam finite model including thickness stretching effect for bending analysis of curved nanobeams", *Mech. Adv. Mater. Struct.*, **26**(7), 614-630. https://doi.org/10.1080/15376494.2017.1410903.

Mohammadimehr, M., Rostami, R. and Arefi, M. (2016), "Electro-elastic analysis of a sandwich thick plate considering FG core and composite piezoelectric layers on Pasternak foundation using TSDT", *Steel. Compos. Struct.*, **20**(3), 513-543. http://doi.org/10.12989/scs.2016.20.3.513.

Mohamed Ali, J.S., Alsubari, S. and Aminand, Y. (2016), "Hygro-thermoelastic analysis of orthotropic cylindrical shells", *Lat. Am. J. Solids Struct.*, **13**, 573-589. https://doi.org/10.1590/1679-78252249.

Ni, Z., Cao, X., Wang, X., Zhou, S., Zhang, C., Xu, B. and Ni, Y. (2021), "Facile synthesis of copper(I) oxide nanochains and the photo-thermal conversion performance of its nanofluids", *Coatings*, **11**, 749. https://doi.org/10.3390/coatings11070749.

Rezaiee-Pajand, M., Masoodi, A.R. and Arabi, E. (2018), "On the shell thickness-stretching effects using seven-parameter triangular element", *Eur. J. Comput. Mech.*, **27**(2), 163-185. https://doi.org/10.1080/17797179.2018.1484208.

Rivera, M.G., Reddy, J.N. and Amabili, M. (2016), "A new twelve-parameter spectral/hp shell finite element for large deformation analysis of composite shells", *Compos. Struct.*, **151**, 183-196. https://doi.org/10.1016/j.compstruct.2016.02.068.

Rivera, M.G. Reddy, J.N. and Amabili, M. (2020), "A continuum eight-parameter shell finite element for large deformation analysis", *Mech. Adv. Mater. Struct.*, **27**(7), 551-560. https://doi.org/10.1080/15376494.2018.1484531.

Shariyat, M. and Alipour, M.M. (2017), "Analytical bending and stress analysis of variable thickness FGM auxetic conical/cylindrical shells with general tractions", *Lat. Am. J. Solids Struct.*, **14**(5). https://doi.org/10.1590/1679-78253413.

Sayyad, A.S. and Ghugal, Y.M. (2018), "Effect of thickness stretching on the static deformations, natural frequencies, and critical buckling loads of laminated composite and sandwich beams", *J. Braz. Soc. Mech. Sci. Eng.*, **40**, 296. https://doi.org/10.1007/s40430-018-1222-5.

Sun, J., Aslani, F., Wei, J. and Wang, X. (2021), "Electromagnetic absorption of copper fiber oriented composite using 3D printing", *Construct. Build. Mater.*, **300**, 124026. https://doi.org/10.1016/j.conbuildmat.2021.124026.

Talebizadehsardari, P., Eyvazian, A., Musharavati, F., Babaei Mahani, R. and Sebaey, T.A. (2020), "Elastic wave characteristics of graphene reinforced polymer nanocomposite curved beams including thickness stretching effect", *Polymers*, **12**(10), 2194. https://doi.org/10.3390/polym12102194.

Tounsi, A., Benguediab, S., Houari, M.S.A. and Semmah, A.W. (2013), "A new nonlocal beam theory with thickness stretching effect for nanobeams", *Int. J. Nanosci.*, **12**(4), 1350025. https://doi.org/10.1142/S0219581X13500257.

Wang, M., Jiang, C., Zhang, S., Song, X., Tang, Y. and Cheng, H. (2018). "Reversible calcium alloying enables a practical room-temperature rechargeable calcium-ion battery with a high discharge voltage". *Nature. Chem.*, **10**(6), 667-672. https://doi.org/10.1038/s41557-018-0045-4.

Xu, X. and Nieto-Vesperinas, M. (2019), "Azimuthal imaginary poynting /momentum density", *Phys. Rew. Lett.*, **123**(23), 233902. https://doi.org/10.1103/PhysRevLett.123.233902.

Yang, M., Li, C., Zhang, Y., Jia, D., Zhang, X., Hou, Y. and Wang, J. (2017). "Maximum undeformed equivalent chip thickness for ductile-brittle transition of zirconia ceramics under different lubrication conditions". *Int. J. Mach. Tool. Manuf.*, **122**, 55-65. https://doi.org/10.1016/j.ijmachtools.2017.06.003.

Yang, Y., Chen, H., Zou, X., Shi, X., Liu, W., Feng, L. and Chen, Z. (2020). "Flexible carbon-fiber/semimetal bi nanosheet arrays as separable and recyclable plasmonic photocatalysts and photoelectrocatalysts", *ACS Appl. Mater. Interface.*, **12**(22), 24845-24854. https://doi.org/10.1021/acsami.0c05695.

Zenkour, A.M. (2016), "Hygrothermal analysis of heterogeneous piezoelectric elastic cylinders", *Math. Models. Eng.*, **2**(1), 1-17.

Zenkour, A.M. (2018), "Generalized thermoelasticity theories for axisymmetric hollow cylinders under thermal shock with variable thermal conductivity", *J. Mole. Eng. Mater.*, **6**(3-4), 1850006. https://doi.org/10.1142/S2251237318500065.

Zenkour, A.M. (2020a), "Thermal-shock problem for a hollow cylinder via a multi-dual-phase-lag theory", *J. Therm. Stresses*, **43**(6), 687-706. https://doi.org/10.1080/01495739.2020.1736966.

Zenkour, A.M. (2020b), "Thermo-diffusion of solid cylinders based upon refined dual-phase-lag models", *Multidisc. Model. Mater. Struct.*, **16**(6), 1417-1434. https://doi.org/10.1108/MMMS-12-2019-0213.

Zenkour, A.M. and Kutbi, M.A. (2020), "Thermoelastic interactions in a hollow cylinder due to a continuous heat source without energy dissipation", *Mater. Res. Express*, **7**, 035702. https://doi.org/10.1088/2053-1591/ab7a61.

Zhao, X., Zhu, W. D. and Li, Y.H. (2020a), "Analytical solutions of nonlocal coupled thermoelastic forced vibrations of micro-/nano-beams by means of Green's functions", *J. Sound. Vib.*, **481**, 115407. https://doi.org/10.1016/j.jsv.2020.115407.

Zhao, N., Deng, L., Luo, D. and Zhang, P. (2020b), "One-step fabrication of biomass-derived hierarchically porous carbon/MnO nanosheets composites for symmetric hybrid supercapacitor", *Appl. Surf. Sci.*, **526**, 146696. https://doi.org/10.1016/j.apsusc.2020.146696.

Zhuo, Z., Wan, Y., Guan, D., Ni, S., Wang, L., Zhang, Z. and Zhang, B.T. (2020), "A loop-based and AGO-incorporated virtual screening model targeting AGO-mediated miRNA–mRNA interactions for drug discovery to rescue bone phenotype in genetically modified mice", *Adv. Sci.*, 7(13), 1903451. https://doi.org/10.1002/advs.201903451.

Zhang, Y., Li, C., Jia, D., Zhang, D. and Zhang, X. (2015), "Experimental evaluation of MoS_2 nanoparticles in jet MQL grinding with different types of vegetable oil as base oil", *J. Clean. Prod.*, **87**, 930-940. https://doi.org/10.1016/j.jclepro.2014.10.027.

Zhang, K., Huo, Q., Zhou, Y., Wang, H., Li, G., Wang, Y. and Wang, Y. (2019), "Textiles/metal–organic frameworks composites as flexible air filters for efficient particulate matter removal", *ACS Appl. Mater. Interface.*, **11**(19), 17368-17374. https://doi.org/10.1021/acsami.9b01734.

AT